Development and Evaluation of Perceptually Adapted Color Gradients

Article *in* Image Processing, IET · June 2013

DOI: 10.1049/iet-ipr.2012.0085

4 authors, including:

Aurora Sáez
Universidad de Sevilla

Begoña Acha
Universidad de Sevilla

Carmen Serrano
Universidad de Sevilla

Development and evaluation of perceptually adapted color gradients for color edge detection

Aurora Sáez, Carlos S. Mendoza, Begoña Acha, Carmen Serrano

Abstract

Although several color edge detectors have been proposed, most of them utilized Euclidean color distances in different color spaces to measure color differences. In this paper a set of color gradients based on color visual perception is proposed. These color gradients are designed in uniform color spaces and use perceptual color difference equations. In order to be able to study the gradients performance, they have been applied in a variational level set formulation. A comparative study has been performed. A set of synthetic images, generated for this purpose, has allowed carrying out an extensive evaluation. Both quantitative and qualitative measures are used. It can be conclude that detectors based on CIE94 color difference equation are the best regarding to the correlation with color visual perception. Our main contributions are: the derivation of perceptual color gradients, the design of a perceptual evaluation with a specific synthetic dataset and the comparison between detectors based on different color differences.

Keywords: perceptual color gradients, perceptual evaluation, color difference equations

1. Introduction

Edge detection is one of the fundamental operations in computer vision. Edges correspond to abrupt discontinuities in physical quantities such as gray-level, color, texture or motion. In order to analyze an image, the human visual system detects changes in it, that is, discontinuities. Nowadays, the majority of the image processing tasks are developed for color images. The advantage of color edge detection schemes over grayscale approaches is easily demonstrated by considering the fact that those edges that exist at the boundary between regions of different colors cannot be detected in grayscale images if there is no change in intensity [1]. The color edge detectors can be classified into two groups: those techniques extended from grayscale edge detectors which apply the detection method in each color plane and combining the results, and those techniques that take into account the vector nature of the color images [2]. Several color edge detectors preserving this vector nature have been proposed [2] but none of them take into account recent advances in measuring perceptual color differences.

Different algorithms that extend the concept of derivative operator to three-color-component pixels have been developed in the literature. One of simplest approximations consists in generalizing the operators based on the first derivative, e.g. Sobel, commonly applied in the grayscale images into the multidimensional case. Wesolkowski compared several edge detectors in multiple color spaces, and he drew the conclusion that the performance of Sobel operator is superior to others [3]. This is the reason why Sobel operator is chosen in this paper. As results correlated with perceptual color differences are intended, RGB space is avoided because it is not a perceptually uniform color space. Instead, we make use of a perceptual uniform color space (CIE $L^*a^*b^*$) and the CIELAB, CIE94 and CIEDE2000 color difference equations [4],[5]. A comparative study between these gradients is carried out. To evaluate the performance of them, a variational Level Set technique where these color gradients control external energies is developed. As the aim is to measure how the detectors are correlated with the human visual perception, an extensive evaluation is performed. A database formed by 96 images has been generated and both quantitative and qualitative measures are used to test the correlation between the detector output and the visually perceived color difference. Other authors have approached to the field of perceptual color edge detectors. However, in their work, there is lack of a thourogh evaluation[6], [7], [8].

The rest of the paper is organized as follows: Section 2 summarizes the color gradients proposed. The variational Level Set technique implemented to evaluate the color gradients is introduced briefly in Section 3. In Section 4 the complete developed method is exposed. The experimental results are explained in Section 5. Some conclusions are presented in Section 6.

2. Color gradients

In this paper several perceptual color gradients are proposed and compared. These color gradients are developed in a uniform color space and preserve the vector nature of the color images in that space.

2.1. Perceptual Uniform Color Space and Color Difference Equations

In 1976, International Commission on Illumination (CIE) standardized $L^*a^*b^*$ space as perceptually uniform [9]. A color space is perceptually uniform if perceptual color differences can be measured with Euclidean distances in this space. The three coordinates of $L^*a^*b^*$ represent the lightness of the color (L^*), its position between red/magenta and green (a^*) and its position between yellow and blue (b^*). It can also be expressed in terms of cylindrical coordinates with the perceived lightness L^*, the chroma C^*_{ab} and the hue h^*_{ab}, defined in (1) and (2) respectively.

$$C_{ab}{}^* = \sqrt{a^{*2} + b^{*2}} \tag{1}$$

$$h_{ab} = arctan\left(\frac{b^{*2}}{a^{*2}}\right) \tag{2}$$

CIELAB color difference, also known as ΔE^*_{ab}, is calculated using (3).

$$\Delta E^*_{ab} = \sqrt{\Delta L^{*2} + \Delta a^{*2} + \Delta b^{*2}} \tag{3}$$

where $\Delta L^* = L^*_1 - L^*_2$ (Δa^* and Δb^* are defined in the same manner for coordinates a^* and b^*).

However, subsequent experiments demonstrated that Euclidean distance ΔE^*_{ab} is not an accurate measure of perceived color difference between two stimuli. To correct the problem a new difference formula was recommended by CIE [4] in 1994.

$$\Delta E_{94}{}^* = \sqrt{\left(\frac{\Delta L^*}{k_L S_L}\right)^2 + \left(\frac{\Delta C^*_{ab}}{k_C S_C}\right)^2 + \left(\frac{\Delta H^*_{ab}}{k_H S_H}\right)^2} \tag{4}$$

$$S_L = 1, \tag{5}$$

$$S_C = 1 + 0.045\, C^*_{ab}\,, \tag{6}$$

$$S_H = 1 + 0.015\, C^*_{ab}\,. \tag{7}$$

The factors k_L, k_C and k_H, are included to match the perception of the background conditions.

Later, CIEDE2000 was developed to correct defficiencies of previous color difference equations [10]. Its accuracy to predict small perceived color differences have been demonstrated [11]

$$\Delta E_{00} = \sqrt{\left(\frac{\Delta L'}{K_L S_L}\right)^2 + \left(\frac{\Delta C'}{K_C S_C}\right)^2 + \left(\frac{\Delta H'}{K_H S_H}\right)^2 + R_T \left(\frac{\Delta C'}{K_C R_C}\right)\left(\frac{\Delta H'}{K_H S_H}\right)} \tag{8}$$

where $\Delta C'$ and $\Delta H'$ are defined in [5].

2.2. Proposed color gradients

In color gradients, the vector nature of color is preserved throughout the computation. Color images are viewed as a two-dimensional three channel vector field. Each channel in this vector is characterized by a discrete integer function $\mathbf{f}(x, y)$. The value of this function at each point is defined by a three dimensional vector in a given color space [2]. Therefore, a pixel is defined as in (9).

$$\mathbf{f}(x, y) = \begin{bmatrix} C_1(x, y) \\ C_2(x, y) \\ C_3(x, y) \end{bmatrix} \tag{9}$$

where $C_i(x, y)$ represents the value of the pixel in the i-th color plane ($i = 1, 2, 3$), and (x, y) refers to the spatial dimensions in the 2-D plane.

The operator based on the firs derivative, commonly applied in the grayscale imaging, is generalized into multidimensional case in [2]. Plataniotis extends the Sobel operator, with the horizontal and vertical masks shown in (10), by constructing the vectors: $\mathbf{H}^+ = \mathbf{f}_7 + 2\mathbf{f}_3 + \mathbf{f}_8$, $\mathbf{H}^- = \mathbf{f}_9 + 2\mathbf{f}_2 + \mathbf{f}_6$, $\mathbf{V}^+ = \mathbf{f}_6 + 2\mathbf{f}_4 + \mathbf{f}_8$, $\mathbf{V}^- = \mathbf{f}_9 + 2\mathbf{f}_5 + \mathbf{f}_7$, according to the notation used in Figure 1. They calculate the color vector gradient as $\mathbf{H}^+ - \mathbf{H}^-$ and $\mathbf{V}^+ - \mathbf{V}^-$, respectively. In order to estimate the color variation in the vertical and horizontal directions, the following scalars are calculated: $\|\mathbf{H}^+ - \mathbf{H}^-\|$, $\|\mathbf{V}^+ - \mathbf{V}^-\|$. The magnitude B of the maximun variation is estimated as:

$B = \sqrt{\|\mathbf{H}^{+} - \mathbf{H}^{-}\|^2 + \|\mathbf{V}^{+} - \mathbf{V}^{-}\|^2}$.

$\mathbf{f}_9$	$\mathbf{f}_5$	$\mathbf{f}_7$
$\mathbf{f}_2$	$\mathbf{f}_1$	$\mathbf{f}_3$
$\mathbf{f}_6$	$\mathbf{f}_4$	$\mathbf{f}_8$

Figure 1: Sliding window

$$X_1 = \begin{bmatrix} -1 & 0 & 1 \\ -2 & 0 & 2 \\ -1 & 0 & 1 \end{bmatrix}, X_2 = \begin{bmatrix} -1 & -2 & -1 \\ 0 & 0 & 0 \\ 1 & 2 & 1 \end{bmatrix} \tag{10}$$

In this paper, we propose calculating the gradient along x and y direction as shown (11) and (12).

$$G_x = \Delta E \left(\mathbf{H}^{+}, \mathbf{H}^{-}\right) \tag{11}$$

$$G_y = \Delta E \left(\mathbf{V}^{+}, \mathbf{V}^{-}\right) \tag{12}$$

where ΔE denotes the color difference between two vectors. Then, the gradient magnitude can be computed as shown in (13).

$$G = \sqrt{G_x^2 + G_y^2} \tag{13}$$

In this paper three color gradients are studied, each one of them is obtained by applying:

- $\mathbf{f}(x, y) = [L^*(x, y), a^*(x, y), b^*(x, y)]$ and ΔE determined by Euclidean distance (CIELAB).
- $\mathbf{f}(x, y) = [L^*(x, y), a^*(x, y), b^*(x, y)]$ and ΔE determined by CIE94 color difference equation.
- $\mathbf{f}(x, y) = [L^*(x, y), a^*(x, y), b^*(x, y)]$ and ΔE determined by CIEDE2000 color difference equation.

3. Variational level set

Once a color gradient is estimated, the simplest edge detector is obtained by thresholding this gradient. In the three proposed color gradient estimators, the dynamic range of the color gradient differs between the three color difference measures. This implies that a different threshold should be chosen to detect edges with the different gradient estimators and the quality of edges detected from each gradient estimator depends strongly on the choice of this threshold. Therefore, in order to make the comparison between the three gradient estimators independent from this choice, a level set formulation has been applied.

Level set methods [12] have been widely used as global approaches towards the optimization of active contours for the segmentation of objects of interest from the background. In these methods, in each time t edges are considered to be in the zero-level of a scalar function $\phi(t)$, called level-set function. The challenge of a level-set algorithm is to make ϕ evolve along t so that its zero level converge at the real boundaries in the image. The general level set equation is presented in (14),

$$\frac{\partial \phi}{\partial t} + F|\nabla \phi| = 0 \tag{14}$$

where F represents the speed function. One of the main challenges in the employment of level set techniques is to overcome the generation of shocks in ϕ, very sharp or flat shape during the evolution, which can result in less than accurate contours. Many authors avoid this problem by re-initializing the function ϕ to a signed function periodically. In this paper, this problem is overcome with the method developed by Li et al [13]. In the reported work, a new term is introduced into (14) to maintain the level set function near the signed distance function, thus avoiding the need for re-initialization of the level set function. It has been shown that the resulting expression is the following gradient flow:

$$\frac{\partial \phi}{\partial t} = \mu \left[\Delta \phi - div \left(\frac{\nabla \phi}{|\nabla \phi|} \right) \right] + \lambda \delta(\phi) div \left(g \frac{\nabla \phi}{|\nabla \phi|} \right) + \nu g \delta(\phi) \tag{15}$$

where μ determines the deviation of ϕ from a signed distance function, λ and ν are the coefficients of the weighted length of the zero level curve and of the weighted area inside the zero level curve respectively, and t is the time step of the experiment.

The second and the third term in the right hand side of (15) are responsible of driving the zero level curve towards the object boundaries. g is the edge indicator function, usually defined as:

$$g = \frac{1}{1 + |\nabla G_\sigma * I|^2} \tag{16}$$

where G_σ is the Gaussian kernel with standard deviation σ and I is the test image.

In the proposed method, the edge indication function g has been modified to:

$$g = \frac{1}{1 + |VD(diff\{I\})|^2} \tag{17}$$

where $diff$ is an anisotropic diffusion filter and VD are the proposed color gradients that are applied to the diffused image. Therefore, modifying the edge indicator function includes two aspects:

- The Gaussian filter smothing is substituted by an color anisotropic diffusion filter [15]. Both smoothing were tested but the color anisotropic diffusion filter obtained better results according experiments.
- Gradients the diffused image are computed with the three proposed color gradients approaches explained in Section 2.

4. Methodology

The data flow diagram in Figure 2 gives an overview of the main steps of the perceptual color detectors based on proposed color gradients.

a. Uniform color space transform. The RGB image is transform in to the uniform color space CIE $L^*a^*b^*$, previously described.

b. Anisotropic diffusion filtering. In the anisotropic diffusion [14] a within-region smoothing is largely performed without blurring between-region boundaries. In this paper an extension of the method to color image is implemented [15], where a separate anisotropic diffusion of chromatic

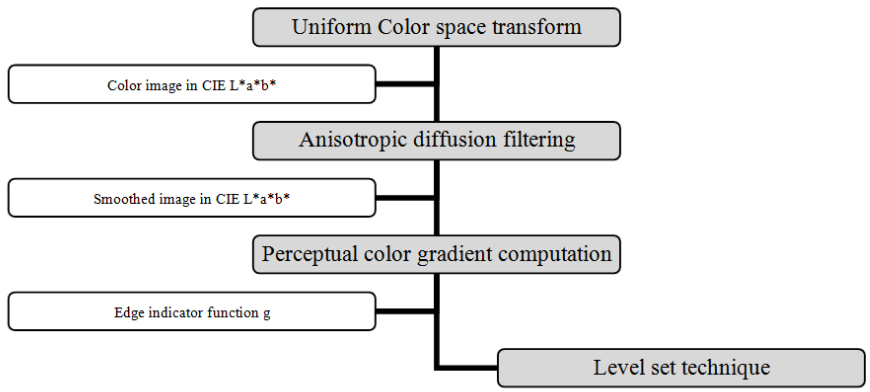

Figure 2: Proposed system

and achromatic channels is performed. This way finds its rationale in the models of color vision: the human visual system senses color information through photoreceptors which can be regarded as three sets of filters tuned to the wavelengths of red, green and blue; this information is then split into chromatic (2-D) and achromatic (1 -D) channels before being further and independently processed. Neurophysiological evidence shows that there exists a perfect agreement between the second Human Visual System processing stage and the opponent-colors theory based on the three antagonistic mechanisms red-green, blue-yellow and black-white. These stimuli can also be conveniently expressed in terms of hue, saturation and lightness. Hue and saturation are processed together using the formalism of phasors: hue is the phase and saturation is the magnitude of a complex function defined as the complex chromaticity. The scalar achromatic information represented by lightness is separately diffused.

c. Perceptual color gradients computation. The proposed color gradients explained in Section 2 are computed from diffused image.

d. Level set technique. The level set formulation explained in Section 3 is applied with the edge indicator function as:

$$g = \frac{1}{1 + |VD(diff\{I\})|^2} \tag{18}$$

where $diff$ is an anisotropic diffusion filter and VD are the proposed color gradients that are applied to the diffused image.

5. Results

A comparative study between the three proposed detectors is carried out to test which one best correlates to color visual perception.

A synthetic database composed by 96 images has been generated to evaluate the performance of the detectors. To this aim, evaluation procedures defined by Zhu et al. [16], have been carried out. Both quantitative and qualitative measures are used. The quantitative performance measures are based on edge deviation from true edges. For this experiment the predefined edge map (ground truth) is required. Since objective measures are not sufficient to model the complexity of human visual systems, a qualitative evaluation has been performed as well. This measure allows us to test which is the correlation between the detector output and visually perceived color differences.

5.1. Images database

A set of 96 color images has been created to evaluate edge detector performance.

In 1978, CIE published guidelines to co-ordinate researchers who study color differences [17]. Five color centers were recommended for study. Our images are based on these centers, which are shown in Table 1.

color	L^*	a^*	b^*	C^*	h
Gray	63.5	-0.6	0.8	0.9	126.4
Red	46.2	37.8	23.8	44.7	32.2
Yellow	87.9	-6.6	46.1	46.5	98.2
Green	58.6	-33.7	0.8	33.7	178.7
Blue	37.3	4.7	-32	32.3	278.3

Table 1: The CIELAB values of color centers

In each image in the database two color centers from Table 1 are present. Along with these two color centers, two additional colors appears in the

(a) (b) (c)

Figure 3: Example of images from the dataset. a) Sample pairs with 0.5 CIELAB units. b) Sample pairs with 4 CIELAB units. c) Sample pairs with 10 CIELAB units.

image. These two additional colors are X CIELAB units distant from those color centers. X is a parameter that varies within the database.

In order to evaluate the ability to detect different edge orientation, rectangular and circular objects have been included in the different images in the database. In Figure 3 an example of three images from the dataset is shown. In Figure 3 a) there is a small square inside the green zone with 0.5 CIELAB units color difference to the green background, and a small one also with 0.5 CIELAB units to the yellow background. It can be observed that the human visual system cannot perceive this difference. Despite the fact that color difference in Figure 3 b) are greater (4 CIELAB value) the small squares are still almost imperceptible. Nevertheless in Figure 3 c), with 10 CIELAB units between samples, they are already perceived by the human visual system.

It is also interesting to note that for two sample pairs with the same CIELAB units between them, visual assessment may be not equal. An example of this approach is illustrated in Figure 4, where the difference in terms of CIELAB units between gray samples is the same than between the blue samples, but they are not representing the same perceptual difference. We perceive more difference between the gray pair than the blue pair. However if this perceptual difference is represented in CIE94 and CIEDE2000 equations, as shown in Table 2, values in CIE94 units and CIEDE2000 units are lower for the blue pair than for the gray pair as human eye perceive them.

More examples of images from dataset are shown in Figure 5.

The aim of this paper is to check if any color edge detector is able to

	CIELAB	CIE94	CIEDE2000
Gray	10	9.613	10.259
Blue	10	4.17	5.6

Table 2: The CIELAB values of color centers

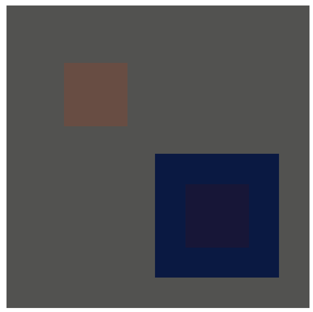

Figure 4: Example of images with same CIELAB units between two pairs but different visual perception

behave like the human eye does.

5.2. Evaluation of results

Two experiments carried out to evaluate the resulting edge maps: a subjective test and a quantitative evaluation measure. The quantitative measure evaluates how much the detected edge deviates from the true edges (since images are synthetic we know the ground truth). The subjective test provides information about how much the edge detection is correlated with the visually perceived color differences.

5.2.1. Subjective test

Subjective evaluation is very important in image processing [14]. Moreover, as the aim of our work is related to visually perceived color differences, this issue becomes essential.

In this evaluation, six observers were asked how many different colors they could distinguish in each image. For each image, the true number of perceived colors was fixed to the most voted. Finally, a detector gets one hit in an image when the number of colors detected in this image coincides with the true number of perceived colors. For example in Figure 6 a), the

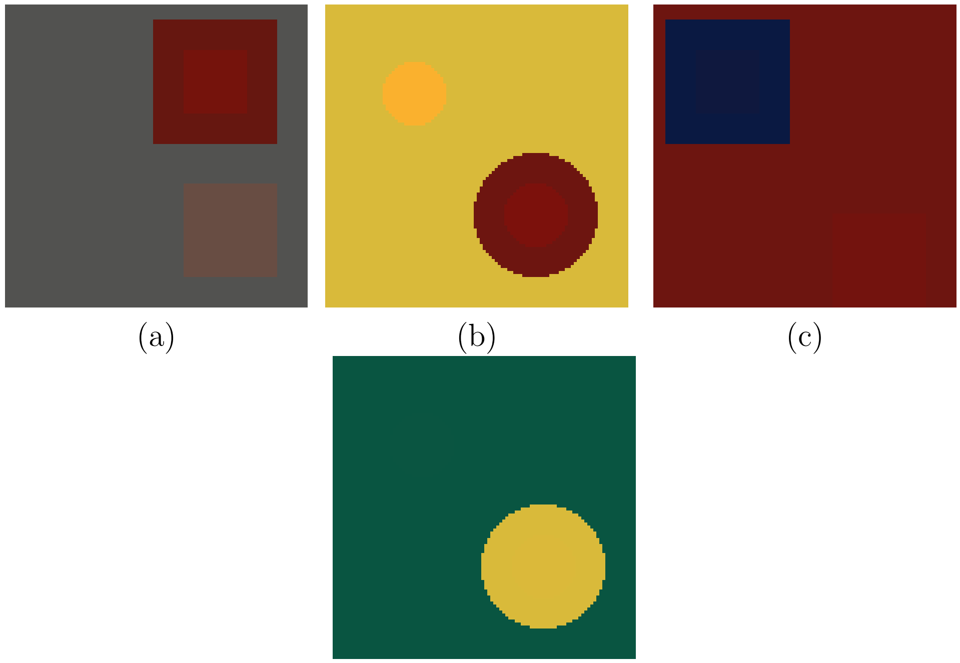

(a) (b) (c) (d)

Figure 5: Example of images from the dataset. a) Sample pairs with 10 CIELAB units. b) Sample pairs with 8 CIELAB units b) Sample pairs with 6 CIELAB units d) Sample pairs with 0.5 CIELAB units

observers distinguished two different colors. The detectors based on CIE94 and CIEDE2000 (Figure 6 c) and d)) detected two different color, however the detector based on Euclidean distance distinguished four colors (Figure 6 b)). Each detector hit ratio is summarized in Table 3.

	Lab	CIE94	CIEDE2000
Hit Ratio	65.54%	80.2%	76.04%

Table 3: Subjective test results.

As shown in Table 3, the detector based on CIE94 has a performance more correlated to human perception. This result contrasts with the fact that CIEDE2000 was developed to improve CIE94. Its rationale can be found in the fact that CIEDE2000 was optimized for small color differences

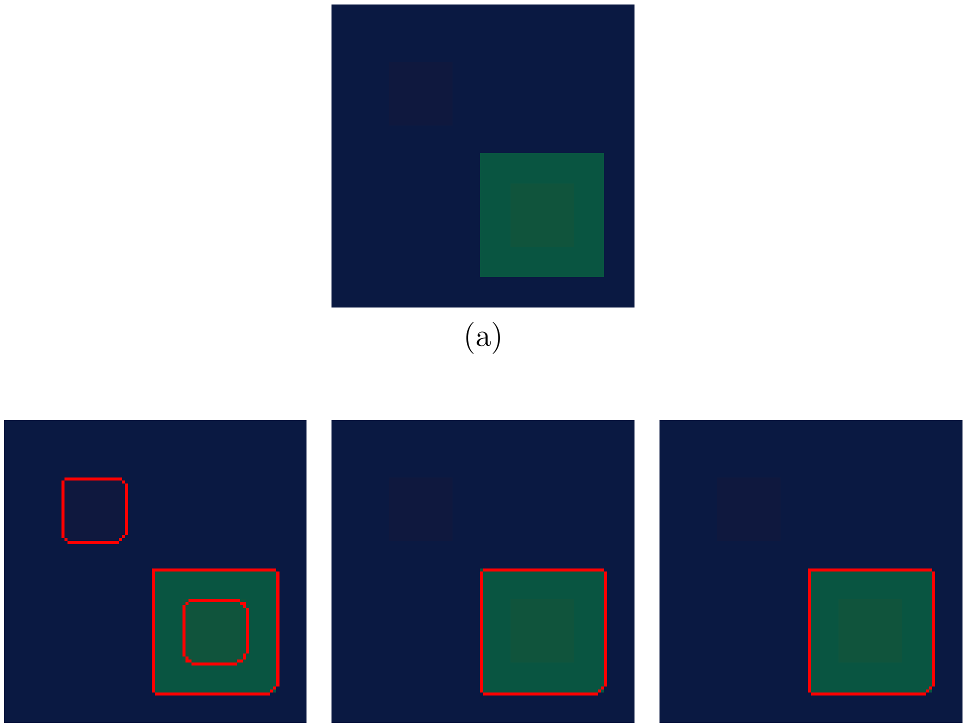

(a)

(b) (c) (d)

Figure 6: a) Test image. b) Output of detector based on CIELAB. c) Output of detector based on CIE94. d) Output of detector on CIEDE2000.

[18] whereas our database contains images whose color differences can not be considered small.

5.2.2. Quantitative measure

An edge map is defined as a binary image were edges are valued 1. The ground-truth edge map is the edge map that contains the real edges. The quantitative evaluation requires the ground-truth edge map. In the proposed evaluation we have distinguished between two ground-truth edge maps: the objective ground-truth edge map, known because the database contains only synthetic images, and the perceived ground-truth edge map, containing edges according to observers' perception. Objective ground-truth edge map and perceived ground-truth edge map differ in some images in the database. This is illustrated in Figure 6. In Figure a) four colors are present but only two are perceived.

We adopted as a quantitative measure to evaluate the three color detectors a figure of merit proposed by Pratt [19]. It is defined as:

$$F_{Pratt} = \frac{\Sigma_{i=1}^{I_D} \left(\frac{1}{1+\alpha d(i)^2} \right)}{max(I_D, I_I)} \tag{19}$$

where I_D is the amount of pixels that the detector considered edges, I_I is the amount of real pixels belonging to an edge, $d(i)$ is the distance between the i-th pixel of the detector edge map and its nearest pixel in the real edge map, a is a scaling constant with usual value 1/9. When F_{Pratt} value is 1, computed edge matches real edge.

As explained above, two measures have been derived from (19). In the objective F_{Pratt}, objective ground-truth edge map are utilized to its evaluation and in the perceived F_{Pratt} edges contained in the perceived ground-truth edge map are utilized to calculate equation (19). Results of the evaluation of F_{Pratt} with both ground-truth edge maps are presented in Table 4. As can be observed, the best result for the perceived F_{Pratt} corresponds to the detector using CIE94 difference equation, as in the subjective test. This is not the case for the objective F_{Pratt}, where the detector based on CIELAB attained the best result.

	CIELAB		CIE94		CIEDE2000	
Objective F_{Pratt}	0.89	0.1361	0.7753	0.1993	0.7688	0.1926
Perceived F_{Pratt}	0.8404	0.1651	0.8832	0.1081	0.869	0.1091

Table 4: The CIELAB values of color centers

Figure 7 shows another example of the detectors performance that illustrates the advantanges of the detector based on CIE94 color difference equations. Observers agreed that they could distinguish a blue circle and a small grayish circle on the gray background. The detector based on CIE94 was the only one which detected the circles according to the observers perception.

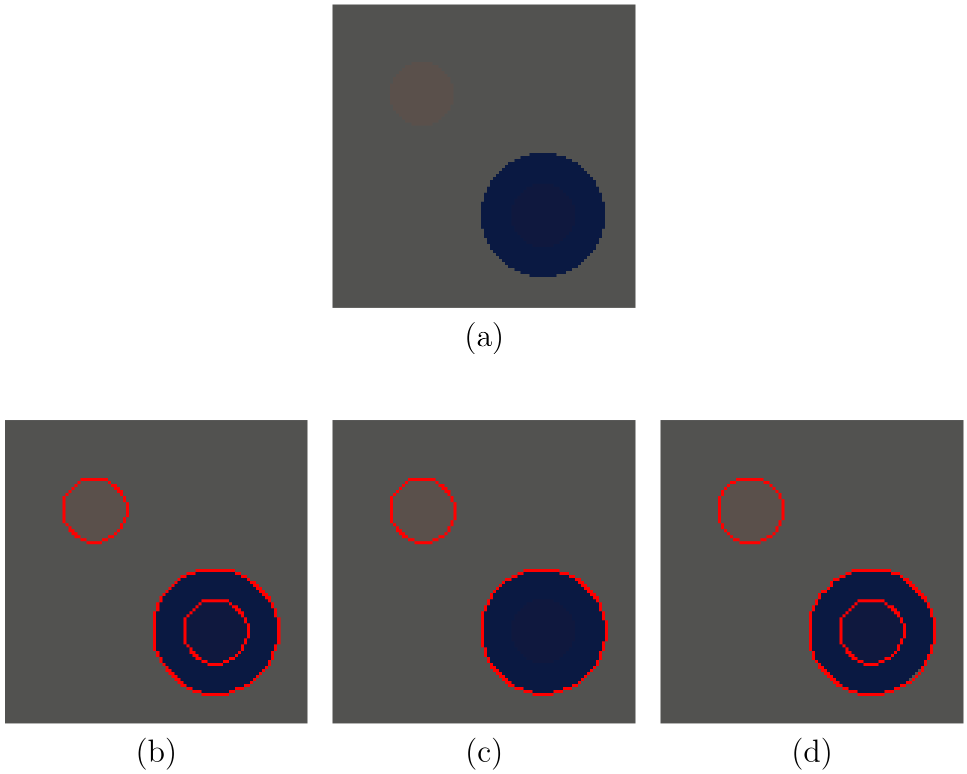

Figure 7: a) Test image. b) Output of detector based on CIELAB. c) Output of detector based on CIE94. d) Output of detector based on CIEDE2000.

6. Conclusions

In this paper three different perceptually adapted color gradients have been proposed. These gradients have been integrated in a level-set framework to color edge detection. This color edge detection algorithm is used to evaluate the three color gradients with two evaluation tests: a subjective test and a quantitative evaluation measure. To this purpose, a synthetic image database following CIE guidelines for coordinated research on color difference evaluation [17] has been developed. The edge detector using the color gradient based on CIE94 resulted the best both according to the subjective test and the perceived quantitative measure (perceived F_{Pratt}). An additional advantage of CIE94 color difference equation is its low computational cost when compared to CIEDE2000 difference equation.

References

[1] A.N. Evans, X.U. Liu, A morphological gradient approach, IEEE Transaction on Image Processing, 15(6) (2006) 1454-1563.

[2] K.N. Plataniotis, A.N. Venetsanopoulos, Color Image Processing and Applications, Springer-Verlag, Berlin, 2000.

[3] S. Wesolkowski, M.E. Jernigan, R.D. Dony, Comparison of color image edge detectors in multiple color space, ICIP, (2009) 796-799.

[4] CIE Publication 116. Industrial color-difference evaluation. Vienna, Austria, 1995.

[5] CIE, Improvement to industrial colour-difference evaluation, CIE Publication 142 (2001), Cnetral Bureau of the CIE, Vienna, 2001.

[6] P. Montesinos, B. Magnier, A new perceptual edge detector in color images, Lecture Notes in Computer Science (including subseries Lecture Notes in Artificial Intelligence and Lecture Notes in Bioinformatics) 6474 LNCS (PART 1), (2010) 209-220.

[7] L. Xue-Wei, X-R. Zhang, A perceptual color edge detection algorithm, Proceedings - International Conference on Computer Science and Software Engineering, 1(4721746) (2008) 297-300.

[8] X. Chen, H. Chen, A novel color edge detection algorithm in RGB color space, International Conference on Signal Processing Proceedings, ICSP , 5655926 (2010) 793-796.

[9] K. McLaren, The development of the CIE 1976 (L*a*b*) uniform colour-space and colour-difference formula, Journal of the Society of Dyers and Colourists, 92 (1976) 338-341.

[10] M.R. Luo, G. Cui, B. Rigg, The development of the CIE 2000 colour-difference formula: CIEDE2000, Color Research and Application 26 (5), (2001) 340-350

[11] G. Cui, M.R. Luo, Testing colour-difference formulae and uniform colour spaces uusing small colour difference datasets, 11th Congress of the International Colour Association (AIC), Sidney, Austrtalia, (2009)

[12] S. Osher, J. A. Sethian, Fronts propagating with curvaturedependent speed - algorithms based on hamilton-jacobi formulations, J Comput Phys, 79 (1998) 12-49.

[13] C. Li, C. Xu, C. Gui, M. D. Fox, Level set evolution without re-initialization: a new variational formulation, IEEE Computer Society Conference on Computer Vision and Pattern Recognition, (2005).

[14] P. Perona, J. Malik, Scale-space and edge detection using anisotropic diffusion, IEEE Trans. PAMI, 12(7) (1990) 629-639.

[15] L. Lucchese, S.K. Mitra, Color segmentation based on separate anisotropic diffusion of chromatic and achromatic channels, IEEE Proceedings Vision, Image and Signal Processing, 148(3) (2001) 141-150.

[16] S.Y. Zhu, K.N. Plataniotis,A.N. Venetsanopoulos, Comprehensive analysis of edge detection in color image processing, Optical Engineering, 38(4) (1999) 612-625.

[17] A.R. Robertson, CIE guidelines for coordinated research on colour-difference evaluation, Color Res. Appl. 3(3) (1987) 149-151.

[18] G. Sharma, W. Wu, E.N. Dalal, The CIEDE2000 color-difference formula: Implementation notes, supplementary test data, and mathematical observations, Color Research and Application, 30(1) (2005) 21-30.

[19] W.K. Pratt, Digital Image Processing, Wiley-Interscience, New York, 1978.